Conference paper

Amey Nimkar, Sandeepan Maity and Shmaryahu Hoz*

Coordination of tridentate ligands to SmI_2: cooperativity and incremental effect on reduction potential and on reactivity

https://doi.org/10.1515/pac-2019-0213

Abstract: The effect of coordination of a series of tridentate ligands (TDLs) on various features of SmI_2 was determined. The TDLs used in this study were diethylene glycol (OOO), diethanolamine (ONO), 2-(2-Aminoethoxy) ethanol (OON), N-(2-Hydroxyethyl) ethylene diamine (ONN) and glycerol (GLY). Of special interest is the effect of these additives on the reduction potential of SmI_2. The cyclic voltammograms of the TDLs with nitrogen at the binding sites display simultaneously several peaks, each corresponding to a different coordination level of SmI_2, enabling determination of three equilibrium constants. The results are in concert with electronic spectra of SmI_2 complexes with these ligands. The second and third equilibrium constants were found to be larger than the first, demonstrating the cooperativity effect. Moreover, the incremental effect of each moiety on the reduction potential of SmI_2 was determined. Regarding reactivity of SmI_2, excessive coordination of some ligands is shown to have an adverse effect.

Keywords: ICPOC-24; kinetics; ligands; reaction mechanisms; reduction; reduction potential; SmI_2.

Introduction

One of the features that render SmI_2 a very popular reducing agent [1–10] is the ability to tailor its properties to the needs by using additives, [11–14] which affect its reactions by three main mechanisms: (a) increasing the reduction potential of SmI_2, (b) prompting efficient unimolecular protonation of the radical anion within the ion pair, and (c) affecting the actual size of SmI_2 and consequently also the size of Sm^{3+}. It should be noted that this classification may be further refined. For example, increasing the steric size of SmI_2 by coordination could change the electron transfer mechanism from inner- to outer-sphere. At the same time, it may also affect the product distribution. For example, steric inhibition to simultaneous binding of two ketyl radicals to Sm^{3+} favors reduction over coupling, and hence also production of alcohol in pinacol-type reactions [15, 16].

One of the most important groups of additives is glycolic ligands (G-ligands). These ligands are various modifications of ethylene glycol (EG) such as di-, tri- and tetra-ethylene glycols, their corresponding ethers, and related derivatives. EG itself effectively coordinates to SmI_2 and significantly enhances its reaction with various substrates [17–20]. Examples of its additional effects on reactions of SmI_2 are the change in facial stereoselectivity in the reduction of norcamphore [21] and the induction of an impressive reaction course change from 1,2-reduction to 1,2-migration in the reaction of SmI_2 with barbituric acids [22]. The study of a series is in general more informative than the study of a single ligand, as it may reveal trends, however only few studies

Article note: A collection of invited papers based on presentations at the 24th IUPAC International Conference on Physical Organic Chemistry (ICPOC 24) held in Faro, Portugal, 1–6 July 2018.

***Corresponding author: Shmaryahu Hoz,** Department of Chemistry, Bar-Ilan University, Ramat Gan 5290002, Israel, e-mail: shoz@mail.biu.ac.il
Amey Nimkar and Sandeepan Maity: Department of Chemistry, Bar-Ilan University, Ramat Gan 5290002, Israel

of series were conducted with G-ligands. Hilmersson found the following order of reactivity in the reactions of SmI_2 with 3-heptanone [17]:

EG < diethylene glycol > triethylene glycol > tetraethylene glycol.

Daasbjerg and Skrydstrup studied the effect of ethers on diastereoselectivity in coupling reactions of benzaldehyde and cyclohexanecarboxaldehyde in the presence of a variety of polyethylene glycols, including derivatives that contain carbohydrates [23]. Flowers *et al.* examined in a similar series the effect of successive replacement of the OH group by an alkoxy group on reactions with benzyl bromide and also determined the crystal structure of SmI_2 coordinated by TDLs of this series [24]. Here, we present a systematic study of a series of G-ligands, focusing mainly on TDLs. The study includes the effect on reduction potential determined by cyclic voltammetry (CV), electronic spectra, and kinetic studies with three substrates, each representing a different class of compounds.

Results and discussion

The TDLs that were studied are shown in Scheme 1. This series is comprised of G-ligands with nitrogen replacing a single oxygen atom, either at the terminal position (OON) or at the central position (ONO). Unfortunately, these ligands often precipitate even at low concentrations with SmI_2, and more so with Sm^{3+}. Precipitation problems are particularly encountered with nitrogen containing ligands. The difficulty becomes more severe when two oxygen atoms are replaced by nitrogen atoms. Nevertheless, in some cases we managed to perform a few studies with low concentration of ligand. To this series we also added two bidentate ligands – OO and ON; in the latter case, N-methylethanolamine was used, as ethanolamine causes abundant precipitation. Also examined is the series HO–X–OH where X is a bridge with varied number of methylene groups. The most relevant member of this series is 1,5PD where the central oxygen is replaced by a methylene unit (OCO).

The substrates chosen for this study were benzyl chloride, anthracene, and cyclohexanone. Benzyl chloride represents a class of substrates where the electron transfer is coupled to the departure of the leaving group and is the rate determining step [25–27]. Anthracene represents a group of substrates that react via outer sphere electron transfer mechanism [28]. The third substrate, cyclohexanone, belongs to the group of substrates that react via inner sphere electron transfer mechanism [29].

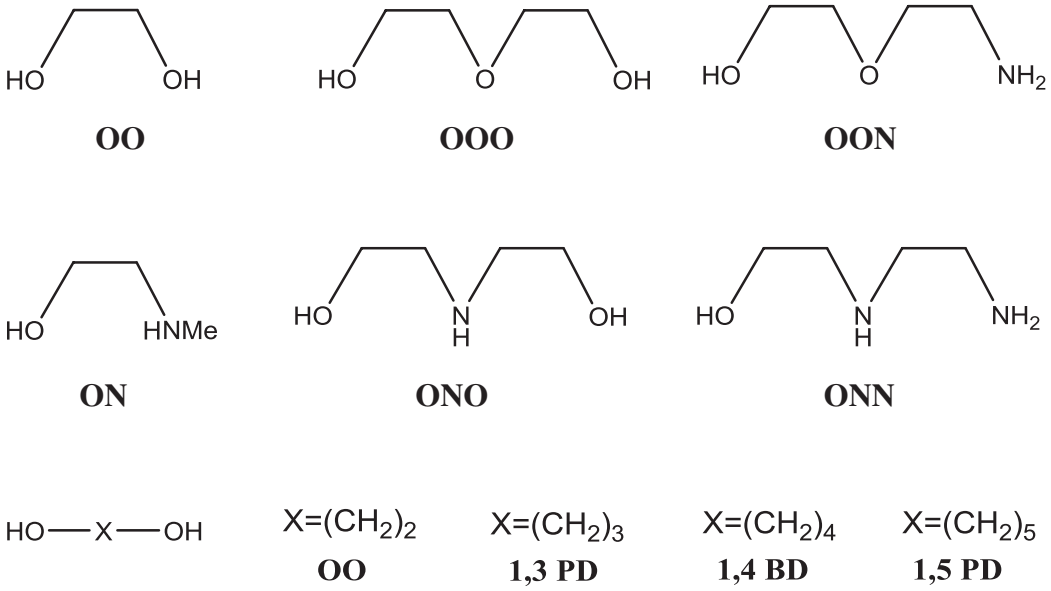

Scheme 1: Structures and notations of ligands used in the current study.

The substrates and their reactions are given in equations 1–3:

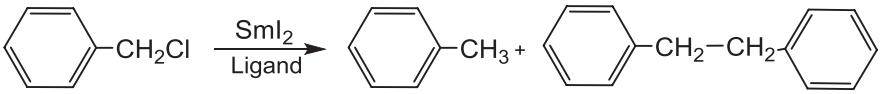

(1)

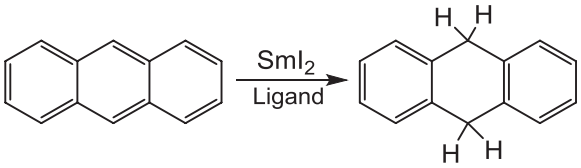

(2)

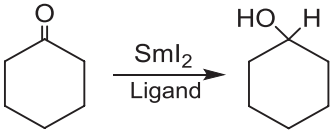

(3)

Electronic spectrum

We begin our discussion with UV spectra of SmI_2 with the four ligands shown in Figure 1 (other spectra are given in the Supplementary material). Clearly, the transformation in the typical double humped spectrum of SmI_2 around 600 nm is the best indication for coordination of the ligand to SmI_2. It is interesting to note that while nearly 0.5 M of MeOH is needed [30] to affect a change in the spectrum of SmI_2, 100-fold smaller concentrations of EG are sufficient (5 mM, see Supplementary material), and for TDLs around 1 mM is already effective. Moreover,

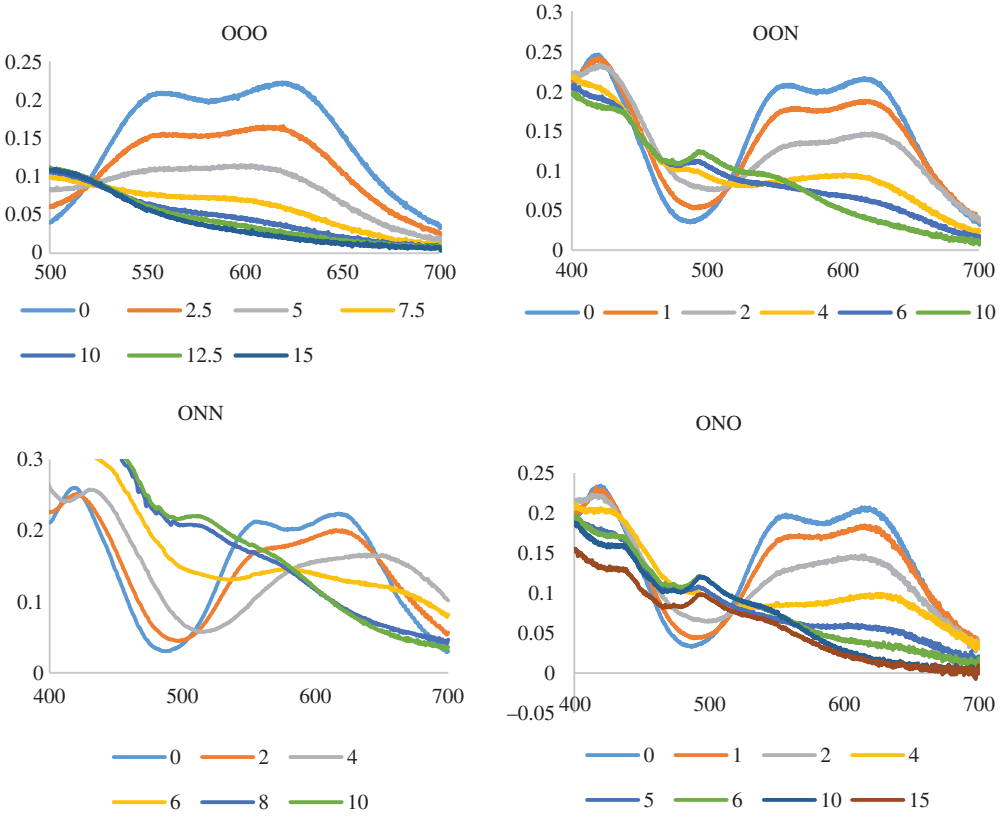

Figure 1: UV-Vis Spectra (OD vs. wavelength nm) for SmI_2 [2 mM] in THF in the presence of OOO, OON, ONO and ONN. [Ligand concentrations are in mM].

saturation, namely complete coordination, is reached for the TDLs in the range of 10–15 mM. Thus, the interaction of the G-ligands with SmI_2 becomes stronger with the number of binding sites. Of special importance are the isosbestic points in the spectra: for a reaction in which A is converted to B, and their corresponding spectra cross at a given wavelength, if no considerable amount of intermediate is accumulated, and there is no side-reaction or further reaction, the absorption at the wavelength of the crossing point remains constant during the A-to-B conversion. While in the spectrum of OOO there is one isosbestic point, the nitrogen-containing TDLs display an unusual pattern of breaking the first isosbestic point, and in some cases there is sequential formation of other discrete, or nearly so, isosbestic points. This is clearly seen in the case of ONN and is highly likely to correlate with sequential addition of ligands to the coordination sphere of SmI_2, as shown in Equations 4–6 (L = ligand).

$$SmI_2 + L \overset{K_1}{\rightleftharpoons} SmI_2 \cdot L \tag{4}$$

$$SmI_2 \cdot L + L \overset{K_2}{\rightleftharpoons} SmI_2L_2 \tag{5}$$

$$SmI_2 \cdot L_2 + L \overset{K_3}{\rightleftharpoons} SmI_2L_3 \tag{6}$$

The mono-, di- and tri-ligated SmI_2 have different molar absorbance at the wavelength of the first isosbestic point. The absence of this behavior in OOO could be explained by the replacement of the oxygen atoms of THF by oxygen atoms of OOO; in the case of the nitrogen-containing ligands ONO, OON and ONN, the THF oxygen atoms bound to the samarium are consecutively replaced by nitrogen atoms, changing the energy levels involved in light absorption. The assumption of triple ligation as the saturation point of TDLs around the SmI_2 is based on the crystal structure of SmI_2 complexed to OOO reported by Flowers et al [24]. It should be noted that ligation of three TDLs leads to a coordination number of nine, as opposed to five THF molecules in a THF solution. This is in line with recent work by Maron and Ramírez-Solís, reporting that at high H_2O concentrations, there are likely 8–9 molecules of water coordinated to SmI_2 [31, 32]. It should be noted that in some of the cases the iodide ions may reside in the second coordination sphere. The abovementioned observations of discerned consecutive ligation will become important in the following discussion of the effect of the ligands on the reduction potential of SmI_2.

Cyclic voltammetry studies

The cyclic voltammetry data is given in Table 1 (additional data appears in the Supplementary material). The ligand effect on the reduction potential of SmI_2 was found to be:

$$NNO > ONO > OON > OOO.$$

Table 1: CV data (V) for the SmI_2 (2 mM) in presence of TDLs.[a]

[TDL] mM	OOO	OON	ONO	ONN
0.0	1.16	1.13	1.13	1.13
0.5	1.44	1.17	1.17	1.21
1.0	1.53	1.21	1.23	1.68
1.5	1.54	1.58	1.80	1.94
2.0	1.55	1.77	1.86	1.96
2.5	1.56	1.82	1.88	1.98
3.0	1.57	1.83	1.88	1.99
3.5	1.58	1.83	1.89	2.00
4.0	1.58	1.90	2.03	2.15
6.0	1.59	1.91	2.05	2.19
10.0	1.61	1.92	2.05	2.19

[a]Expressed with positive sign for convenience.

We have recently pointed out that replacement of oxygen by nitrogen atoms in the binding sites of a ligand increases its affinity to SmI_2 [33]. As the reduction potential reflects the energy difference between Sm^{2+} and Sm^{3+}, the finding that replacement of oxygen by nitrogen also strongly increases the reduction potential suggests that this replacement causes even stronger binding to Sm^{3+} than to Sm^{2+} [34, 35].

It should be noted that the incremental increase in reduction potential due to N/O replacement is not additive: replacement of terminal oxygen induces an increase of 0.31 V, while replacement at the central position leads to an increase of 0.44 V. Yet, replacement of two oxygens (ONN) does not yield a 0.75 V increase, but rather a smaller increase of 0.58 V.

The CVs of nitrogen-containing TDLs display a unique phenomenon not observed with any of the other ligands. A very close analysis of the voltammograms reveals simultaneous appearance of several peaks, resulting from various complexation levels. This is more prominent with ONN, but is discernible also with ONO and OON. Figure 2 shows that with ONN, already at a concentration of 1.5 mM, peaks corresponding to mono-, di- and tri-ligation are observed. This is more clearly seen at a concentration of 4 mM.

With single nitrogen – ONO and OON – this could also be seen, however at some concentrations magnification of the figure is needed in order to determine the exact location of the peaks, as demonstrated in the Supplementary material. Thus, the coexistence of free SmI_2, as evidenced by the peak around –1.1 V, along with peaks corresponding to multi-ligations, indicates a cooperative effect. Namely, the ligands prefer to join a samarium cation, which already carries a ligand molecule, rather than to coordinate to free SmI_2. Assuming that the current intensity is proportional to the concentration of samarium entities in solution, it is possible to determine the equilibrium constants of Equations 4–6. The data is presented in Table 2, along with standard deviations based on determination of equilibrium constants at several ligand concentrations.

Due to interpenetration of the peaks, the standard deviations are large, in particular for OON. Nevertheless, the data clearly shows that, K_2 is larger than K_1. In addition, regardless of the numerical values of the equilibrium constants, the appearance of the second and third ligand peaks, alongside the large peak corresponding to free SmI_2, clearly indicates a preference for ligating to the already coordinated SmI_2. This phenomenon of cooperativity [36] was also suggested by Flowers for the second equilibrium constant of HMPA with SmI_2 [37]. At this stage, it is not clear whether this is a general phenomenon common to many ligands, which is not always detectable, or perhaps it is unique to large ligands such as HMPA or TDLs. A possible cause for this phenomenon is two processes affecting the coordination ΔG: removal of THF molecules from SmI_2 and coordination of the incoming ligand, which is accompanied by a gain in free energy.

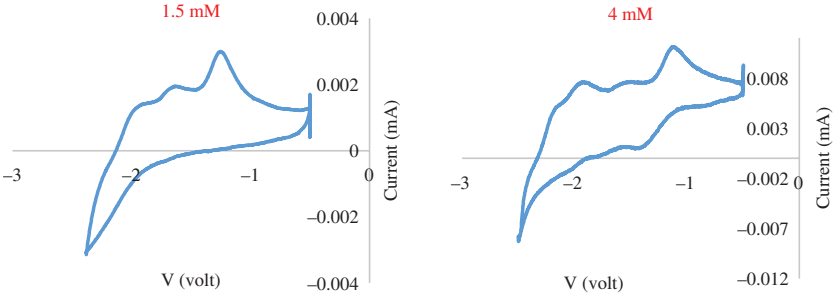

Figure 2: Cyclic voltammograms of SmI_2 (2 mM) in THF in presence of ONN.

Table 2: Equilibrium constants for successive ligand attachment to SmI_2.

	K_1 M^{-1}	K_2 M^{-1}	K_3 M^{-1}
OON	405 ± 280	718 ± 391	N/A
ONO	209 ± 32	444 ± 95	313 ± 120
ONN	376 ± 64	630 ± 29	445[a]

[a]Single determination.

Table 3: Reduction potentials (V) with 1–3 ligands attached to SmI_2.

	$SmI_2 \cdot L$	$SmI_2 \cdot L_2$	$SmI_2 \cdot L_3$
OON	1.55	1.77	1.92
ONO	1.55	1.82	2.05
ONN	1.57	1.92	2.19

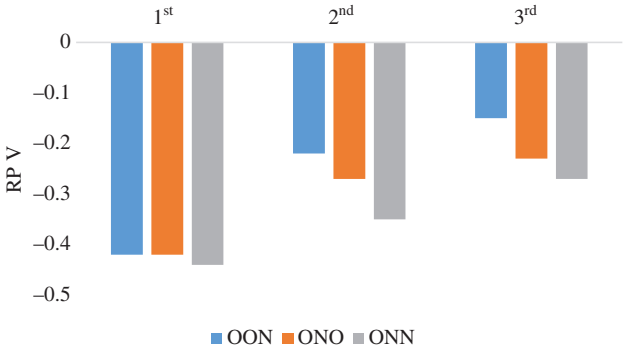

Figure 3: Incremental changes in reduction potential (RP) with addition of 1st, 2nd and 3rd ligand molecules to SmI_2.

Thus, if the first ligand molecule, due to spatial demands, causes detachment of additional THF molecules, the second ligand molecule does not have to displace as many THF molecules as the first one, leading to net energy gain.

The unique structure of the CVs enables, for the first time, the determination of the incremental effect on the reduction potential of each ligand that is added to the coordination sphere. The data is given in Table 3.

It turns out that the effect of the first molecule added to SmI_2 on the reduction potential is independent of its structure, as all three ligands give about the same reduction potential of 1.55 V. The difference between the three ligands begins to develop with the addition of the second ligand, and it grows in the order: ONN > ONO > OON. This follows the coordination ability of these ligands to SmI_2. However, as mentioned above, the coordination to Sm^{2+} is only half of the story. The second part is the coordination to Sm^{3+}, as it is the energetic difference between the two which governs the reduction potential [34]. It is interesting to note that the major contribution to the reduction potential is made by the first molecule to coordinate to SmI_2, and it decreases with additional ligands, as shown in Figure 3, which depicts the incremental contributions to the reduction potential.

Kinetics

The kinetics of the reactions was followed by monitoring the disappearance of SmI_2 at 619 nm using a stopped-flow spectrometer. The pseudo first order rate constants at maximal ligand concentration are given in Table 4 (all data is provided in the Supplementary material).

Although the kinetics of the reactions was monitored using stopped-flow UV-Vis spectroscopy due to the rapid precipitation, it was not possible to reach very high concentrations of TDLs. As anticipated, precipitation was more pronounced with the slower reactions, and therefore in the relatively slow reaction of anthracene with ONN, no rate constants could be determined, even at low concentrations.

Of special interest are the reactions with benzyl chloride. Unlike the other substrates, there is a sharp increase in the rate constants, reaching a maximum, followed by a drop (Figure 4). For ONN the maximum could not be reached, as it affects precipitation more vigorously than the other TDLs.

Table 4: Pseudo first order rate constants for SmI_2 reaction with the three substrates in THF.[a]

	Benzyl chloride		Anthracene		Cyclohexanone	
	Conc. mM	$k\ s^{-1}$	Conc. mM	$k\ s^{-1}$	Conc. mM	$k\ s^{-1}$
MeOH	500	0.0025	500	0.014	500	0.011
OO	250	0.0094	250	0.015	250	0.095
ON	72	9.7	72	58	20	258
OOO	15	0.0042[b]	10	0.012	10	0.13
OON	5	4.4[b]	10	70	10	140
ONO	15	0.0042[b]	10	131	10	52
ONN	4	27[b]	NA	NA	4	93

[a]$[SmI_2] = 2$ mM, [substrate] = 10 mM. [b]Non-maximal rate constant.

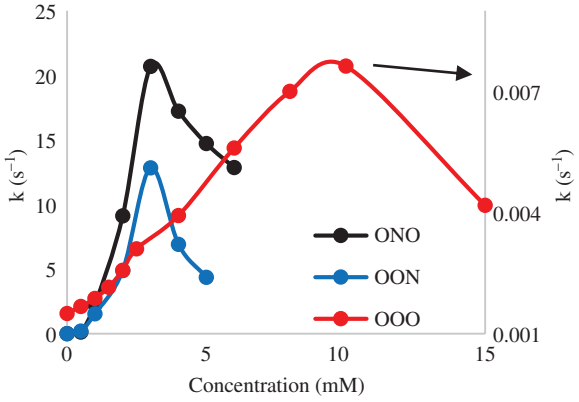

Figure 4: Effect of TDLs concentration on the pseudo first order rate constants of the reactions of benzyl chloride with SmI_2 (2 mM).

This behavior was observed previously for the reaction of benzyl chloride with SmI_2 [28, 38] and is probably due to the need for electrophilic assistance in expulsion of the chloride ion into the THF medium. Thus, on the one hand, addition of the TDLs to SmI_2 increases the reduction potential and therefore enhances the rate of the electron transfer step. But on the other hand, engulfing the Sm^{3+} by these ligands prevents the direct contact required between Sm^{3+} and the chloride ion. As can be seen in Table 3, the incremental increase in reduction potential upon going from 2 to 3 ligands is relatively small, and therefore obstruction of the electrophilic assistance plays a more dominant role. Overall, addition of a third molecule to the coordination sphere leads to rate retardation. Namely, the maximum rate constant is due to $SmI_2 \cdot L_2$, and the rate decreases with its conversion to $SmI_2 \cdot L_3$.

It is noteworthy that in the reaction of anthracene, the same order of reactivity is obtained as in the reaction of benzyl chloride: ONN > ONO > OON > ON > OOO > OO, as well as the same ligand effect on the reduction potentials. The similarity between the two substrates is interesting, because benzyl chloride reacts by an inner sphere mechanism, and anthracene reacts by an outer sphere electron transfer mechanism. Surprisingly, in the reactions with cyclohexanone, which like benzyl chloride is an inner sphere electron transfer substrate, the order in the ligands that contain nitrogen is reversed to ON > OON > ONO. Namely, ON, the least active among the three ligands, becomes the most active, replacing ONO at the top of the reactivity scale. The faster reactions of ligands with terminal nitrogen hints at the possibility that the terminal amine attacks the carbonyl to form an imine; imines are well known to react with SmI_2 orders of magnitude faster than carbonyls [39]. Indeed, incubating cyclohexanone with OON for 20 min in THF gave, according to H NMR analysis, 25 % of the Schiff base, and it is highly likely that the presence of the Lewis acid SmI_2 significantly enhances the reaction.

Unlike the other TDLs, OOO did not show any fine structure in the CVs that could be correlated with different degrees of coordination. Yet, in its reaction with benzyl chloride, it displayed the same kinetic pattern, namely reaching a maximal rate constant with increasing concentration, followed by a moderate drop. It was therefore of interest to further investigate this ligand; we compared it with another ligand having three oxygen atoms – glycerol (GLY). As shown in Figure 5, although both ligands eventually reach the same reduction potential, OOO reaches its maximum at much lower concentrations of around 3 mM, whereas the graph for GLY levels off only around 30 mM. This suggests that like the nitrogen-containing TDLs, OOO also has higher equilibrium constants for the second and third ligation with respect to the first one.

Surprisingly, with all three substrates, GLY reacts much faster than OOO (Figure 6) despite its lower affinity to SmI_2.

Thus, for example, at a concentration of 4 mM, the ratio k_{GLY}/k_{OOO} is 2.6 for benzyl chloride, 2 for anthracene, and 11.8 for cyclohexanone. This is even more surprising, considering that at this concentration, the reduction potential for OOO is –1.58 V, while for GLY it is only –1.28 V. This demonstrates once again that in SmI_2 reductions, boosting the reduction potential by an additive may not be the most important factor. It is clear why GLY is faster than OOO in inner-sphere electron transfer reactions, i.e. with benzyl chloride and cyclohexanone, as it coordinates to SmI_2 less efficiently than OOO, and therefore some open sites on SmI_2 are left for coordination with the substrate. However, GLY also showed enhanced reactivity relative to OOO towards anthracene, a substrate known to react by an outer sphere electron transfer mechanism, where direct contact with the substrate is not needed. It is possible that the rate enhancement in this case results from the higher ability to protonate the radical anion of anthracene. This could be attributed in part to a

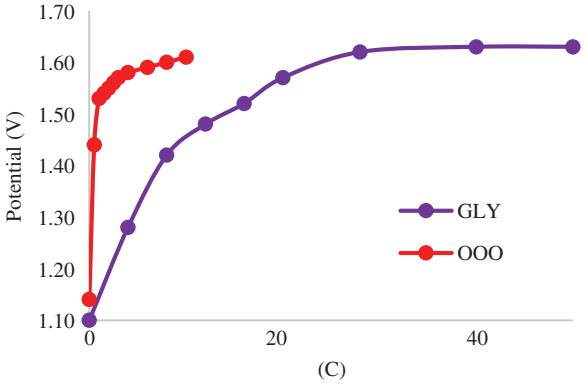

Figure 5: Effect of OOO and GLY on the reduction potential of SmI_2 [*x* axis in mM].

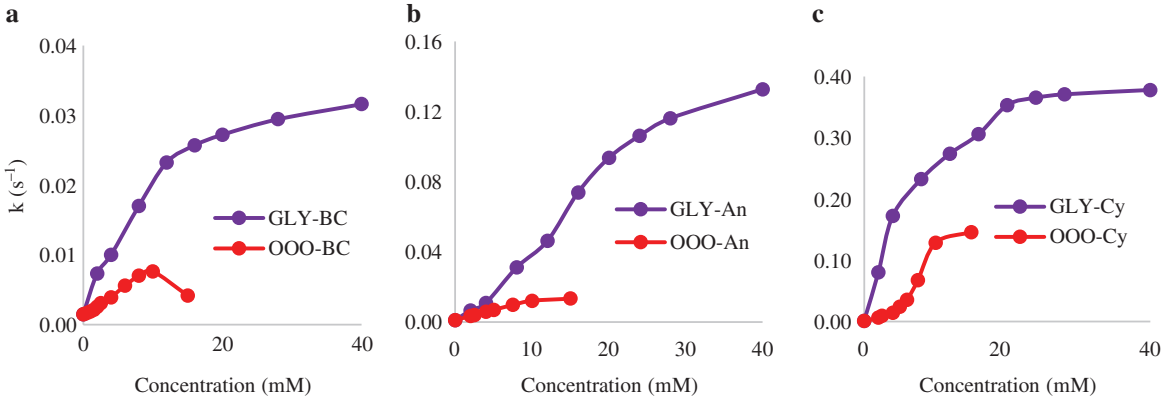

Figure 6: Comparison of pseudo first order rate constants for OOO and GLY with (a) benzyl chloride, (b) anthracene, and (c) cyclohexanone.

statistical factor – the three protons in GLY vs. the two protons in OOO. In addition, it is possible that GLY is more acidic than OOO due to hydrogen bonding by the neighboring OH groups (Scheme 2), which is unlikely for OOO. Such a situation is often encountered with diacids such as malonic or maleic acid, where the second proton stabilizes the carboxylate function through an internal hydrogen bond [40, 41].

Thus, if the central proton of GLY is transferred to the radical anion of anthracene or cyclohexanone, the central oxygen atom has three lone pairs: one interacts with the samarium cation, while the other two form hydrogen bonds with the two neighboring hydroxyl groups. Cyclohexanone therefore benefits twice from having GLY as an additive rather than OOO, as it both enables an inner-sphere electron transfer and enhances protonation.

Finally, we looked into the series HO–X–OH, as one of its members – 1,5PD (OCO) – resembles the TDL series in the number of heavy atoms. It turns out that 1,5PD had no effect on any of the measured parameters: UV, CV or kinetics. Nevertheless, it was interesting to see the effect of the length of the chain bridging the two binding sites on the coordination to SmI_2. We found that 1,5PD did not affect the Vis spectrum or the reduction potential, and 1,4BD had a small effect on both properties (see Supplementary material). The only member of the series beyond EG that showed some interaction with SmI_2 was 1,3PD. Its effect of the reactivity of SmI_2 toward the three substrates was smaller than that of OO (see Supplementary material), although the final effect on the reduction potential was about the same (~1.6 V). Interestingly, while OO displays a sharp rise in the CV, the slope with 1,3PD is much more moderate (Figure 7).

We note that, based on the effect on the Vis spectrum, the affinity to SmI_2 varies in the following order: OO > 1,3PD > 1,4BD > 1,5PD (Supplementary material). Thus, as the bridging chain gets longer, the affinity to SmI_2 decreases, as if the chain entails a dead weight on the two terminal binding sites of this series. The dead weight in this case is paid for in coins of entropy. It is clear that the much weaker binding to SmI_2 of two molecules of MeOH, compared with OO, stems from an entropic origin, as both have the same number of binding sites and heavy atoms. In binding two molecules of MeOH, translational and rotational entropies are paid twice, as opposed to once in EG, giving an advantage to the latter. Within the series of bridged bidentates, the entropy loss is associated mainly with bond rotation. Taking the common value of 4.5 e.u. for each rotationally frozen bond [42] added to the bridge, the penalty in free energy for 1,3PD, 1,4BD and 1,5PD relative to EG is 1.35, 2.7 and 4.05 kcal/mol, respectively. The equivalent reduction factors in the binding equilibrium

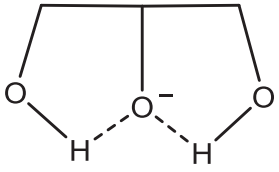

Scheme 2: Hydrogen bonding in glycerol anion.

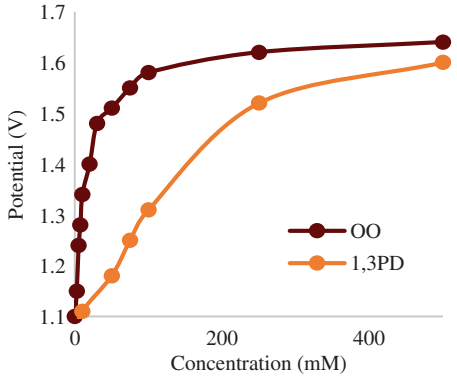

Figure 7: Reduction potential (in absolute values) of OO and 1,3PD as function of ligand concentration.

constant of EG at room temperature are 9.5, 90 and 850. Thus, it is indeed likely that the binding of 1,5PD to SmI_2 would be prohibited by this entropic obstacle.

Experimental section

General

Unless otherwise stated, all regents were purchased from Sigma-Aldrich (Israel) and purified by standard purification procedures. Tetrahydrofuran (THF) was dried over sodium-benzophenone and freshly distilled under argon atmosphere before use. SmI_2 was freshly prepared under inert atmosphere prior to use by reacting samarium metal with diiodoethane in THF at room temperature [43]. SmI_2 concentrations were determined by UV spectroscopy [33] ($\lambda = 619$ nm). All spectral, kinetics and CV experiments were carried out with clean and dry glassware under inert atmosphere.

CV measurements

Single potentiostat – a Bio Logic Scientific instrument was used for CV experiments. Glassy carbon, $Ag/AgNO_3$ in acetonitrile and Pt wire were used as working, reference and counter electrodes, respectively. The potential of $Ag/AgNO_3$ was 0.54 V with respect to SHE. After each measurement, the glassy carbon working electrode was polished with commercial alumina solution, and the Pt wire was thoroughly cleaned with THF. Tetrabutyl ammonium hexafluorophosphate (0.1 M) was used as supporting electrolyte. The concentration of SmI_2 in all measurements was 2 mM.

UV and kinetics measurements

UV and kinetics measurements were performed in a stopped-flow spectrometer. UV-visible spectra of SmI_2 with all ligands were recorded by taking two syringes – one with SmI_2 (2 mM) and the other with ligand – and mixing them in stopped flow.

In kinetics experiments, all reactions were performed under pseudo first order conditions ($[SmI_2] = 2$ mM and [substrate] = 10 mM), and rate constants were monitored by following the disappearance of the absorbance of the SmI_2-additive complex at 619 nm. Reduction of benzyl chloride resulted in a mixture of toluene and 1,2-diphenylethane [28]. Reduction of anthracene and cyclohexanone yielded 9,10-dihydroanthracene [28] and cyclohexanol [44], respectively.

Conclusions

The systematic study of a series of TDLs carried out in this research yielded several interesting results: (1) in the group of nitrogen-containing TDLs, the equilibrium constant for complexation to SmI_2 of the first, second, and in two cases also the third ligand molecules, was determined from cyclic voltammetry (Table 1). (2) A cooperativity effect was demonstrated, as the first ligand coordinated to SmI_2 increased the affinity of consecutive ligand molecules toward SmI_2. This was also directly observed from the cyclic voltammograms in which the peaks of the second and third ligand molecules are seen, in spite of the fact that there is still a large concentration of free SmI_2. (3) CV measurements also enabled to determine the effect of each ligation on the reduction potential of SmI_2. The largest effect is produced by the first molecule that coordinates to

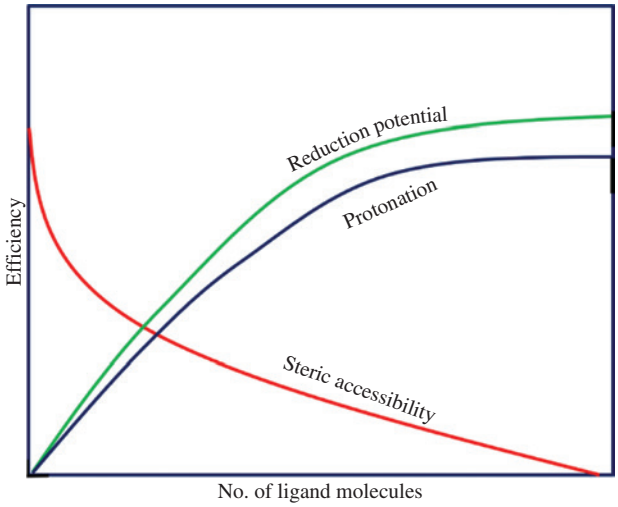

Figure 8: Effect of coordination number on factors that affect the reaction rate.

SmI_2, and the effect decreases as coordination progresses. (4) It was reconfirmed that SmI_2 is more azaphilic than oxophilc. (5) The ascribed course of ligation is in line with the appearance/disappearance of isosbestic points in the Vis spectra. (6) Examination of the reactivity pattern, especially the comparison between OOO and GLY, showed that high ligand affinity to SmI_2, causing sharp increase in reduction potential, rather than a moderate one, is not always beneficial. Figure 8 shows schematically the effect of consecutive addition of ligand molecules to SmI_2, which affect the reduction potential, the rate of protonation within the ion pair when applicable, and the steric effect, which can change the reaction mechanism from an inner-sphere to an outer-sphere electron transfer. Thus, the optimal position along the *x*-axis in Figure 8 is substrate-dependent and should be tailored by either controlling the ligand/SmI_2 ratio, or by erudite choice of ligand, as in the case of OOO vs. GLY (Figures 5 and 6).

Acknowledgement: This research was supported by the Israel Science Foundation (grant no. 583/15).

References

[1] G. A. Molander, C. R. Harris. *Chem. Rev*. **96**, 307 (1996).
[2] G. A. Molander, C. R. Harris. *Tetrahedron* **54**, 3321 (1998).
[3] D. J. Edmonds, D. Johnston, D. J. Procter. *Chem. Rev*. **104**, 3371 (2004).
[4] J. M. Concellon, H. Rodriguez-Solla. *Eur. J. Org. Chem*. **2006**, 1613 (2006).
[5] J. M. Concellon, H. Rodriguez-Solla, C. Concellon, V. del Amo. *Chem. Soc. Rev*. **39**, 4103 (2010).
[6] D. J. Procter, R. A. Flowers II, T. Skrydstrup. *Organic Synthesis using Samarium Diiodide: A Practical Guide*, Royal Society of Chemistry Publishing, UK (2010).
[7] M. Szostak, M. Spain, D. Parmar, D. J. Procter. *Chem. Commun*. **48**, 330 (2012).
[8] M. Tori, M. Sono. *Heterocycles* **89**, 1369 (2014).
[9] X. Just-Baringo, D. J. Procter. *Acc. Chem. Res*. **48**, 1263 (2015).
[10] M. P. Plesniak, H. Huang, D. J. Procter. *Nat. Rev.* **1**, 77 (2017).
[11] A. Dahlen, G. Hilmersson. *Eur. J. Inorg. Chem.* **2004**, 3393 (2004).
[12] R. A. Flowers II. *Synlett* **10**, 1427 (2008).
[13] S. Shi, M. Szostak. *Molecules* **22**, 2018 (2017).
[14] S. Shi, M. Szostak. *Org. Lett*. **17**, 5144 (2015).
[15] R. S. Miller, J. M. Sealy, M. Shabangi, M. L. Kuhlman, J. R. Fuchs, R. A. Flowers II. *J. Am. Chem. Soc.* **122**, 7718 (2000).
[16] H. Farran, S. Hoz. *Org. Lett.* **10**, 865 (2008).
[17] A. Dahlen, G. Hilmersson. *Tetrahedron Lett.* **42**, 5565 (2001).
[18] A. Tarnopolsky, S. Hoz. *J. Am. Chem. Soc.* **129**, 3402 (2007).

[19] M. Levy, S. Hoz. *J. Am. Chem. Soc.* **131**, 8280 (2009).
[20] D. V. Sadasivam, J. A. Teprovich Jr., D. J. Procter, R. A. Flowers II. *Org. Lett.* **12**, 4140 (2010).
[21] S. K. Upadhyay, S. Hoz. *J. Org. Chem.* **76**, 1355 (2011).
[22] M. Szostak, M. Spain, B. Sautier, D. J. Procter. *Org. Lett.* **16**, 5694 (2014).
[23] H. L. Pedersen, T. B. Christensen, R. J. Enemærke, K. Daasbjerg, T. Skrydstrup. *Eur. J. Org. Chem.* **1999**, 565 (1999).
[24] J. A. Teprovich Jr., M. N. Balili, T. Pintauer, R. A. Flowers II. *Angew. Chem. Int. Ed.* **46**, 8160 (2007).
[25] C. P. Andrieux, A. L. Gorande, J.-M. Saveant, *J. Am. Chem. Soc.* **114**, 6892 (1992).
[26] H. Jensen, K. Daasbjerg. *J. Chem. Soc. Perkin Trans.* **2**, 1251 (2000).
[27] O. Yitzhaki, S. Hoz. *Chem. Eur. J.* **21**, 9242 (2015).
[28] S. Maity, S. Hoz. *Chem. Eur. J.* **21**, 18394 (2015).
[29] R. J. Enemærke, K. Daasbjerg, T. Skrydstrup. *Chem. Commun.* **4**, 343 (1999).
[30] A. Yacovan, S. Hoz. *J. Am. Chem. Soc.* **118**, 261 (1996).
[31] X. Zhao, L. Perrin, D. J. Procter, L. Maron. *Dalton Trans.* **45**, 3706 (2016).
[32] A. Ramírez-Solís, J. I. Amaro-Estrada, J. Hernández-Cobos, L. Maron. *J. Phys. Chem. A* **121**, 2293 (2017).
[33] S. Maity, R. A. Flowers II, S. Hoz. *Chem. Eur. J.* **23**, 17070 (2017).
[34] S. Maity, A. Nimkar, S. Hoz. *J. Org. Chem.* **84**, 1994 (2019).
[35] S. Halder, S. Hoz. *J. Org. Chem.* **79**, 2682 (2014).
[36] A. S. Mahadevi, G. N. Sastry. *Chem. Rev.* **116**, 2775 (2016).
[37] J. B. Shotwell, J. M. Sealy, R. A. Flowers II. *J. Org. Chem.* **64**, 5251 (1991).
[38] T. V. Chciuk, W. R. Anderson Jr., R. A. Flowers II. *Angew. Chem. Int. Ed.* **55**, 6033 (2016).
[39] C. N. Rao, S. Hoz. *J. Am. Chem. Soc.* **133**, 14795 (2011).
[40] H. B. Evans, J. H. Goldstein. *Spectrochimica Acta* **24A**, 73 (1968).
[41] M. Merchan, F. Tomas, I. Nebot-Gil. *J. Mol. Struct.* **109**, 51 (1984).
[42] Modern Physical Organic Chemistry, E. V. Anslyn, D. A. Dougherty. University Science Books Publications, California. 71 (2006).
[43] P. Girad, J. L. Namy, H. B. Kagan. *J. Am. Chem. Soc.* **102**, 2693 (1980).
[44] T. V. Chciuk, W. R. Anderson Jr., R. A. Flowers II. *J. Am. Chem. Soc.* **138**, 8738 (2016).

Supplementary Material: The online version of this article offers supplementary material (https://doi.org/10.1515/pac-2019-0213).